RESEARCH ARTICLE

Novel *PRKD* Gene Rearrangements and Variant Fusions in Cribriform Adenocarcinoma of Salivary Gland Origin

Ilan Weinreb,[1,2]* Lei Zhang,[3] Laxmi MS Tirunagari,[3] Yun-Shao Sung,[3] Liang-Chun Chen,[3] Bayardo Perez-Ordonez,[1,2] Blaise A Clarke,[1,2] Alena Skalova,[4] Simion I Chiosea,[5] Raja R Seethala,[5] Daryl Waggott,[6] Paul C Boutros,[6] Christine How,[7,8,9] Fei-Fei Liu,[7,8,9] Jonathan C Irish,[10] David P Goldstein,[10] Ralph Gilbert,[10] Nasir ud Din,[11] Adel Assaad,[12] Jason L Hornick,[13] Lester DR Thompson,[14] and Cristina R Antonescu[3]*

[1]Department of Pathology, University Health Network, Toronto, ON, Canada
[2]Department of Laboratory Medicine and Pathobiology, University of Toronto, Toronto, ON, Canada
[3]Department of Pathology, Memorial Sloan-Kettering Cancer Center, New York, NY
[4]Department of Pathology, Charles University in Prague, Faculty of Medicine, Plzen, Czech Republic
[5]Department of Pathology, University of Pittsburgh Medical Center, Pittsburgh, PA
[6]Informatics and Bio-computing Program, Ontario Institute for Cancer Research, Toronto, ON, Canada
[7]Ontario Cancer Institute, University Health Network, Toronto, Canada
[8]Department of Medical Biophysics, University of Toronto, Toronto, Canada
[9]Department of Radiation Oncology, Princess Margaret Cancer Centre and University of Toronto, Toronto, Ontario
[10]Department of Otolaryngology-Head and Neck Surgery/Surgical Oncology, Princess Margaret Cancer Centre, University Health Network, Toronto, ON, Canada
[11]Department of Pathology, Aga Khan University Hospital, Karachi, Pakistan
[12]Department of Pathology, Virginia Mason Hospital & Seattle Medical Center, WA
[13]Department of Pathology, Brigham &Women's Hospital and Harvard Medical School, Boston, MA
[14]Department of Pathology, Woodland Hills Medical Center, Woodland, CA

Polymorphous low-grade adenocarcinoma (PLGA) and cribriform adenocarcinoma of minor salivary gland (CAMSG) are low-grade carcinomas arising most often in oral cavity and oropharynx, respectively. Controversy exists as to whether these tumors represent separate entities or variants of one spectrum, as they appear to have significant overlap, but also clinicopathologic differences. As many salivary carcinomas harbor recurrent translocations, paired-end RNA sequencing and FusionSeq data analysis was applied for novel fusion discovery on two CAMSGs and two PLGAs. Validated rearrangements were then screened by fluorescence in situ hybridization (FISH) in 60 cases. Histologic classification was performed without knowledge of fusion status and included: 21 CAMSG, 18 classic PLGA, and 21 with "mixed/indeterminate" features. The RNAseq of 2 CAMSGs showed *ARID1A-PRKD1* and *DDX3X-PRKD1* fusions, respectively, while no fusion candidates were identified in two PLGAs. FISH for *PRKD1* rearrangements identified 11 additional cases (22%), two more showing *ARID1A-PRKD1* fusions. As *PRKD2* and *PRKD3* share similar functions with *PRKD1* in the diacylglycerol and protein kinase C signal transduction pathway, we expanded the investigation for these genes by FISH. Six additional cases each showed *PRKD2* and *PRKD3* rearrangements. Of the 26 (43%) fusion-positive tumors, there were 16 (80%) CAMSGs and 9 (45%) indeterminate cases. A *PRKD2* rearrangement was detected in one PLGA (6%). We describe novel and recurrent gene rearrangements in *PRKD1–3* primarily in CAMSG, suggesting a possible pathogenetic dichotomy from "classic" PLGA. However, the presence of similar genetic findings in half of the indeterminate cases and a single PLGA suggests a possible shared pathogenesis for these tumor types.

INTRODUCTION

Salivary gland cancers are diverse and numerous subtypes have been described with important clinical and biological implications. They show significant morphologic overlap and this distinction can be problematic on small biopsies of head and neck tumors. A particularly enigmatic tumor category is the so-called polymorphous low-grade adenocarcinoma (PLGA), which was first described by Evans and Batsakis (1984). PLGA

Conflict of interest: none

Additional Supporting Information may be found in the online version of this article.

Supported by: P01CA47179 (CRA); Grant number: P50 CA 140146-01 (CRA).

*Correspondence to: Ilan Weinreb, University Health Network, 200 Elizabeth Street, Toronto, ON, Canada, M5N-1N7. E-mail: ilan.weinreb@uhn.ca or Cristina R Antonescu, Memorial Sloan-Kettering Cancer Center, 1275 York Ave, New York, NY 10021. E-mail: antonesc@mskcc.org

Received 13 March 2014; Accepted 29 May 2014

DOI 10.1002/gcc.22195

Published online 00 Month 2014 in Wiley Online Library (wileyonlinelibrary.com).

usually arises in the oral cavity, particularly in the palate and can show a wide range of morphologic patterns. It has been described to show "polymorphous architecture with uniform cytology." The main differential diagnoses for PLGA includes pleomorphic adenoma and adenoid cystic carcinoma, with both of these tumor types also frequently arising in the palate. This morphologic overlap is due to the shared cribriform and tubular growth in all three entities. This distinction is not merely academic as pleomorphic adenoma is benign, while adenoid cystic carcinoma has a high mortality rate. Conversely, PLGA is malignant but rarely causes death due to disease (Perez-Ordonez et al., 1998; Castle et al., 1999). PLGA also has a different clinical behavior with occasional cervical lymph node metastases, but only very rare hematogenous spread (Evans and Batsakis, 1984). Adenoid cystic carcinoma shows the opposite pattern.

Controversy has arisen as to whether PLGA represents a single pathologic entity or whether it should be regarded as a spectrum of tumors with extensive morphologic overlap. The large variety of growth patterns seen in PLGA would suggest a potential "waste basket" diagnosis. Some have argued for exclusion of papillary cases from the PLGA category due to their more aggressive course. Recently, a new entity was described in salivary gland, which most likely was previously regarded as PLGA, under the names "cribriform adenocarcinoma of the tongue (CAT)" (Michal et al., 1999) and presently as "cribriform adenocarcinoma of minor salivary gland (CAMSG)." The latter was based on a follow up paper highlighting the wider spectrum of oral cavity sites of origin (Skalova et al., 2011). This tumor was not originally included in the 2005 World Health Organization classification of head and neck tumors as a separate category, but mentioned as a pattern of PLGA that may or may not represent a unique entity (Luna and Wenig, 2005). CAMSG shows solid sheets and nests with slit-like spaces and nuclei reminiscent of papillary thyroid cancer and does not show the architectural diversity attributed to PLGA (Michal et al., 1999; Skalova et al., 2011).

There have been no recurrent molecular abnormalities reported in either PLGA or CAMSG. Occasional nonrecurrent cytogenetic findings have been found in PLGA with some potential overlap with adenoid cystic carcinoma (Martins et al., 2001). Recently, we and others have identified specific fusion transcripts in other salivary gland cancers, including mucoepidermoid carcinoma (Tonon et al., 2003), adenoid cystic carcinoma (Persson et al., 2009), mammary analogue secretory carcinoma (Skalova et al., 2010), and hyalinizing clear cell carcinoma (Antonescu et al., 2011). It can be speculated that tumors with monomorphic cytomorphology in the PLGA/CAMSG spectrum are likely candidates for similar recurrent fusion events. To investigate this hypothesis and interrogate the pathogenetic relationship of tumors included in this morphologic spectrum, next generation RNA sequencing was used on PLGA and CAMSG for novel fusion discovery.

MATERIAL AND METHODS

The institutional pathology files of the authors were searched for the diagnosis of "polymorphous low-grade adenocarcinoma (PLGA)" and "cribriform adenocarcinoma of minor salivary gland (CAMSG)". Hematoxylin and eosin (H&E) stained slides were available for review and were reclassified (IW). Tumors were classified as "classic PLGA" ($n = 18$) when they exhibited a combination of short fascicles, cribriform structures, and a targetoid arrangement of cords of cells around blood vessels and/or nerves. Cases were classified as CAMSG ($n = 21$) when they showed a combination of solid nests and sheets of cells with slit-like or punched out rounded lumina, papillary structures, and a glomeruloid arrangement of cells. Cytologically, CAMSG displayed nuclei with more open or vesicular chromatin. In addition, a subset of lesions was grouped in the "indeterminate" or "mixed" category ($n = 21$). These included cases within the PLGA spectrum but showing mixed or unusual morphology (e.g., basaloid nests, apocrine tubules, canalicular-like areas, and so forth). Many of the cases sent in as PLGA by collaborators ended up being reclassified into the "indeterminate" category. Only cases that were largely papillary were reclassified from PLGA to CAMSG and this is based on the current observation (by IW) that papillary structures are more common in CAMSG than previously appreciated. All cases reclassified as other salivary gland carcinomas or as "adenocarcinoma, not otherwise specified" were excluded from the study.

Fluorescence In Situ Hybridization (FISH)

FISH was performed on 4-μm-thick sections of formalin-fixed paraffin-embedded tissue on all 60 cases. This was performed using custom bacterial artificial chromosome (BAC) probes, flanking the *PRKD1*, *PRKD2*, *PRKD3*, *ARID1A*, and *DDX3X*

genes in separate assays. The BAC clones were obtained from BACPAC sources of Children's Hospital of Oakland Research Institute (CHORI; Oakland, CA) (http://bacpac.chori.org) and were chosen according to the USCS genome browser (http://genome.uscs.edu; Supporting Information Table 1). DNA from individual BACs was isolated according to the manufacturer's instructions and labeled with different fluorochromes in a nick translation reaction (Antonescu et al., 2010). They were then denatured, hybridized to pretreated unstained coated slides, incubated, washed, and mounted with DAPI in an antifade solution, as previously described (Antonescu et al., 2010). The genomic location of each BAC set was verified by hybridizing them to normal metaphase chromosomes. Two hundred nonoverlapping nuclei were scored using a Zeiss fluorescence microscope (Zeiss Axioplan, Oberkochen, Germany), controlled by Isis 5 software (Metasystems, Watertown, MA). A case was confirmed as positive for rearrangement when $\geq$20% of the nuclei examined showed a break-apart signal pattern.

RNA Sequencing

Total RNA was prepared for RNA sequencing in accordance with the standard Illumina mRNA sample preparation protocol (Illumina), as previously described (Antonescu et al., 2013). Briefly, mRNA was isolated with oligo(dT) magnetic beads from total RNA (2 μg) extracted from the index cases. The mRNA was fragmented by incubation at 94°C for 2.5 min in fragmentation buffer. To reduce the inclusion of artifactual chimeric transcripts due to random priming of transcript fragments into the sequencing library because of inefficient A-tailing reactions that lead to self-ligation of blunt-ended template molecules, an additional gel size-selection step (capturing 350–400 bp) was introduced prior to the adapter ligation step (Quail et al., 2008). The adaptor-ligated library was then enriched by PCR for 15 cycles and purified. The library was sized and quantified using DNA1000 kit (Agilent) on an Agilent 2100 Bioanalyzer according to the manufacturer's instructions. Paired-end RNA sequencing at read lengths of 51 bp was performed with the HiSeq 2000 (Illumina). Across the four samples, a total of about 261 million paired-end reads were generated.

Analysis of RNA Sequencing Results with FusionSeq

All reads were independently aligned with STAR alignment software against the human genome reference sequence (hg19) and a splice junction library, simultaneously (Dobin et al., 2013). The mapped reads were converted into Mapped Read Format (Habegger et al., 2011) and analyzed with FusionSeq (Sboner et al., 2010) to identify potential fusion transcripts. The FusionSeq algorithm is a computational method successfully applied to paired-end RNA-seq data for the identification of chimeric fusion transcripts (Antonescu et al., 2013; Mosquera et al., 2013). Briefly, paired-end reads mapped to different genes are first used to identify candidate chimeric transcripts. A cascade of filters, each taking into account different sources of noise in RNA sequencing results, is then applied to remove spurious fusion transcript candidates. A confident list of fusion candidates is generated and they are statistically ranked to prioritize the experimental validation. In this case, the DASPER score was used (difference between the observed and analytically calculated expected SPER): a higher DASPER score indicates a greater likelihood that the fusion candidate is authentic and did not occur randomly. See Sboner et al. (2010) for further details about FusionSeq.

Reverse Transcription Polymerase Chain Reaction (RT-PCR)

An RNA aliquot of the CAMSG index cases (SA2 and SA6) was used for RT-PCR to confirm the novel fusion transcripts. The RNA quality was determined by Eukaryote Total RNA Nano Assay and cDNA quality was tested for PGK housekeeping gene (247 bp amplified product). RT-PCR was performed using the advantage 2 PCR kit (Clonetech, Mountain View, CA). For case SA2 RT-PCR was run for 29 cycles at a 64.5°C annealing temperature, using the following primers: *ARID1A* exon 1 fwd: 5′-CATGGCCTCGCAGTGTTGGG-3′ and *PRKD1* exon 12 rev: 5′-CCAAACTGTCCAGAACCCAG-3′). For case SA6, the RT-PCR was run at 64.5°C annealing temperature for 31 cycles, using the following primers: *DDX3X* exon 7 fwd: 5′-CATGGGAAACATTGAGCTTACTCG-3′ and *PRKD1* exon 14 rev: 5′-CCTGCCCTTTTCACT TGACAAG-3′. The PCR product was confirmed by Sanger sequencing.

Functional Studies to Define the Oncogenic Role of Recurrent ARID1A-PRKD1 Fusion, Including Its Expression into Normal Human Salivary Gland Cell Line

Full length cDNA fusion *ARID1A-PRKD1* was amplified from index patient SA2 using forward

ARID1A (5′-GCAACGGTCCGACCATGGCCGC GCAGGTCGCCCCCGC-3′) and reverse *PRKD1* (5′-GCAACGGTCCGACCATGGCCGCGCAGG TCGCCCCCGC-3′) primers. The amplified DNA was digested with *Rsr*II and *Xho*1 (New England Biolabs, Ipswich, MA) restriction enzymes and cloned into a modified pCD510B vector with a FLAG tag on the N-terminus (a generous gift from Dr. Arul Chinnaiyan). Lentivirus was produced by cotransfecting either pCD510B-*ARID1A-PRKD1* construct or the empty vector along with the helper plasmids psPAX2 and pVSVG (Addgene, Cambridge, MA). Collected and concentrated viral supernatant (40 and 64 hrs after transfection) was used to transduce NIH-3T3 cells or normal salivary gland epithelial cells (HPAM1), purchased from ATCC (Manassas, VA), in the presence of 8 μg/ml of Polybrene (Sigma-Aldrich, St. Louis, MO). Cells were then treated with puromycin (4 μg/ml, Life Technologies, California, CA) 48 hrs after transduction to obtain stable resistant cells. The HPAM1 cells were grown in keratinocyte Basal Media (Lonza, Allendale, NJ) supplemented with KGM SingleQuots (Lonza) on collagen IV coated dishes (BD Bioscience, San Jose, CA).

Additionally, 293FT cells were transfected with the *ARID1A-PRKD1* construct or the empty vector using calcium phosphate. After 24 hrs, cells were split and treated with puromycin (3 μg/ml) after 48 hrs to obtain stable resistant cells.

Gene Expression Analysis by Quantitative PCR and Immunoblotting of ARID1A-PRKD1 Oncoprotein in fusion-expressing HPAM1 Salivary Gland Cells

Total RNA was isolated from tissue culture cells using RNeasy kit (Qiagen, Valencia, CA) and reverse-transcribed using the TaqMan reverse transcription kit (Life Technologies). Predesigned TaqMan Gene Expression Assays and TaqMan Universal PCR master mix (Life Technologies) were used on a ViiA^{TM} 7 Real-Time PCR machine (Life Technologies). Fifteen nanograms of cDNA was used for each sample, and each sample was run in triplicates. GAPDH was used as an endogenous control and the relative expression of genes was calculated using ΔΔCt method (Life Technologies).

Protein lysates were extracted from one *ARID1A-PRKD1* positive SA2 sample as well as from the HPAM1 cell line with and without expression of *ARID1A-PRKD1* fusion. Electrophoresis and Immunoblotting were done using 30 μg of the lysate following standard protocols. Rabbit polyclonal antibodies for PRKD1 (Cell Signaling, Danvers, MA, catalog # 2052; 1:2,000 dilution) and B-actin (cell signaling, 1:1,000 dilution) were used for detection.

RESULTS

Histological and Clinical Findings

A total of 60 cases of "polymorphous low-grade adenocarcinoma (PLGA)" and "cribriform adenocarcinoma of minor salivary gland (CAMSG)" were selected. The patients with available clinical information included 43 females and 17 males, with a wide age-range at diagnosis of 24–84 years (mean 61 years). The tumors occurred in the palate ($n = 27$), buccal mucosa ($n = 7$), lip ($n = 6$), base of tongue ($n = 5$), maxilla/alveolus ($n = 4$), nasopharynx ($n = 3$), parotid ($n = 2$), and 1 each in the tonsil, floor of mouth, mobile tongue, and nasal cavity. In two cases, the anatomic location was not available, but appeared to be oral mucosa and oropharynx histologically. The tumors ranged from 0.7 to 5.0 cm (mean 2.5 cm). The tumors were reclassified into three groups including those that showed "classic PLGA" morphology ($n = 18$), "classic CAMSG" ($n = 21$), and "indeterminate/mixed morphology" ($n = 21$; Fig. 1). The classic PLGA group generally consisted of short fascicles of tumor and a targetoid arrangement of some of the nests around blood vessels or nerves (Figs. 1A and 1B). The classic CAMSG cases showed sheets and large nests of tumor with slit-like or rounded glandular spaces (Fig. 1C). These lacked the hyalinized material of the cribriform areas of classic PLGA, but instead were either empty or had pink homogenous secretions, mucoid material, or extravasated red blood cells. The tumors often had pseudopapillary and glomeruloid formations (Fig. 1D). The tumor nuclei were generally optically clear, although this was not striking in every case. The final category of "indeterminate/mixed" was a heterogenous group that fit the description of the PLGA spectrum but had mixed features, or focal unusual morphology such as canalicular ribbons. All tumors had minimal mitotic activity (<3 MF/10 HPFs) and were low grade.

Follow up and treatment was not available on many cases due to: (1) the number of consult cases, (2) biopsy only cases, and (3) loss to follow up in this cohort. Among the CAMSG group there

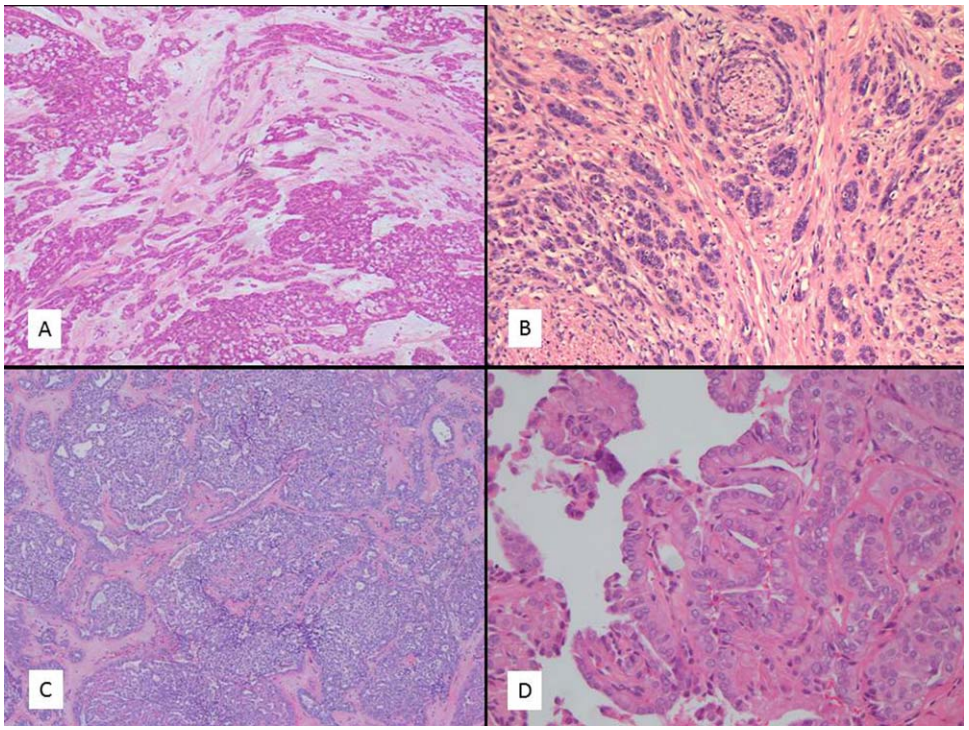

Figure 1. Index cases analyzed by sequencing highlighting the morphologic differences from classic PLGA (A, B) and CAMSG (C, D). The PLGA cases typically show cribriform and fascicular growth (A) with hyalinized basement membrane-like material in the cribriform spaces. Often targetoid arrangement around nerves is seen in these cases (B). CAMSG shows solid nests with slit-like spaces (C) and occasional focal or even diffuse pseudopapillary growth (D). Note the optically clear nuclei in figure D. [Color figure can be viewed in the online issue, which is available at wileyonlinelibrary.com.]

were eight cases known to have a neck dissection, of which seven showed lymph node metastases, often multiple and large. Most of the classic PLGAs did not have a neck dissection, however, the information was incomplete and this may represent a selection/referral bias where smaller biopsies and excisions represented consults. Management details for these patients were often unavailable.

Novel ARID1A-PRKD1 and DDX3X-PRKD1 Fusions Identified by RNA-seq and FusionSeq

The samples with frozen material (SA2 and SA6) were subjected to RNA sequencing to identify potential fusion candidates (Figs. 2 and 3). An *ARID1A-PRKD1* fusion transcript was selected by FusionSeq as the top candidate with a DASPER score of 1.56 in SA2 and a *DDX3X-PRKD1* fusion transcript was selected for SA6 with a DASPER score of 1.34. Read alignments suggested a fusion of *ARID1A* exon 1 on chromosome 1 with *PRKD1* exon 12 on chromosome 14 (Fig. 2A) for SA2 and fusion of *DDX3X* exon 7 on chromosome X to *PRKD1* exon 11 in SA6 (Fig. 3A). RT-PCR confirmed the presence of a fusion transcript of *ARID1A* exon 1 to exon 12 of *PRKD1* in SA2 and *DDX3X* exon 7 to exon 11 of *PRKD1* in SA6. No equivalent t(1;14)(p36.11;q12) or t(X;14)(p11.4;q12) has been described by conventional cytogenetics in PLGA or any other salivary gland tumor to our knowledge, and these chromosomal breakpoints are not listed in the Mitelman database for cytogenetics findings (http://cgap.nci.nih.gov/Chromosomes/Mitelman).

Fluorescence In Situ Hybridization (FISH)

All 60 cases were then investigated for both *ARID1A* and *PRKD1*. Three cases, including the index case SA2, were confirmed to have gene rearrangements in both *ARID1A* and *PRKD1*. All three showed classic CAMSG morphology (Fig. 2B). An additional CAMSG case showed *ARID1A* break-apart alone without *PRKD1*. The index case SA6 with the *DDX3X-PRKD1* fusion predicted by sequencing and RT-PCR was further confirmed to have FISH rearrangements in both *DDX3X* and *PRKD1* and showed classic CAMSG morphology. However, this case also had interesting trabecular areas with a "tall cell" appearance to the cells (Fig. 3B). Nine additional cases with

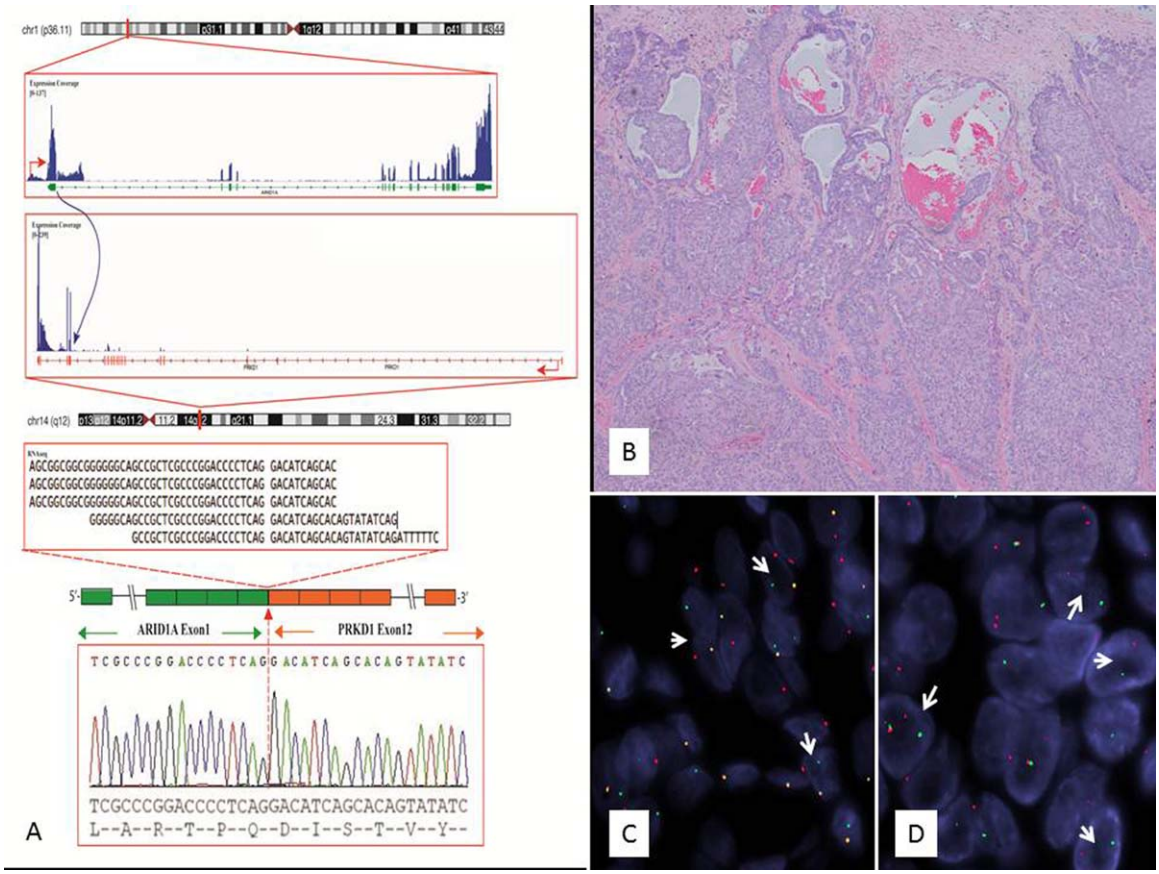

Figure 2. *ARID1A-PRKD1* gene fusion in a base of tongue cribriform adenocarcinoma of minor salivary gland origin (SA2). (A) Schematic representation of the *ARID1A-PRKD1* fusion indicating the loci that are joined together; *ARID1A* exon 1 being fused to *PRKD1* exon 12 (top image). RNA reads covering the fusion junction were isolated independent to FusionSeq analysis work flow, supporting the *ARID1A-PRKD1* fusion candidate (middle image); experimental validation of the fusion by RT-PCR shows the junction sequence between exon 1 of *ARID1A* and exon 12 of *PRKD1* (bottom image); (B) The index case SA2 showed typical morphology with solid growth, slit-like spaces, and glomeruloid structures containing mucoid material; (C, D) Fluorescence in situ hybridization (FISH) for *PRKD1* (C) and *ARID1A* (D) shows break-apart signals with one normal fused yellow signal and separate 5′ green and 3′ red signals indicating rearrangement of the respective gene (arrows). [Color figure can be viewed in the online issue, which is available at wileyonlinelibrary.com.]

PRKD1 rearrangement were identified, four showing classic CAMSG morphology, and five being in the indeterminate/mixed features category (Fig. 4). These could not be classified more specifically. Most of the positive cases showed classic break-apart signals; however, two of the *PRKD1* rearranged tumors showed a signal pattern consistent with an intrachromosomal rearrangement and one showed a signal pattern consistent with an unbalanced translocation with loss of 5′ *PRKD1* material. None of the cases in the "classic PLGA" category showed abnormalities of these genes. A total of 14 cases showed evidence of a rearrangement in one or both of these genes (14/58; 24%); with all except one case showing *PRKD1* gene rearrangement (22%). Two cases failed FISH testing.

As the *PRKD1* gene shares biologic function with *PRKD2* and *PRKD3*, these genes were further investigated by FISH as well. *PRKD2* testing showed six additional positive cases (6/45; 13%). These cases included three classic CAMSG cases, two indeterminate, and one PLGA. In hindsight, this last case showed unusual canalicular ribbons and hemorrhage-filled microcystic spaces not typically seen in PLGA in addition to the more traditional fascicular and targetoid areas. *PRKD3* rearrangement was found in six additional cases (6/38; 16%), representing four classic CAMSG and two indeterminate cases (Fig. 5).

Of the fusion-positive cases (Table 1), the tumors arose in a slightly younger group of patients as compared to the total with a range of 24–84 years (mean 59.0 years); approximately 4 years younger than the fusion-negative group ranging from 27 to 83 (mean 63 years). The fusion-positive cases occurred over a wide site

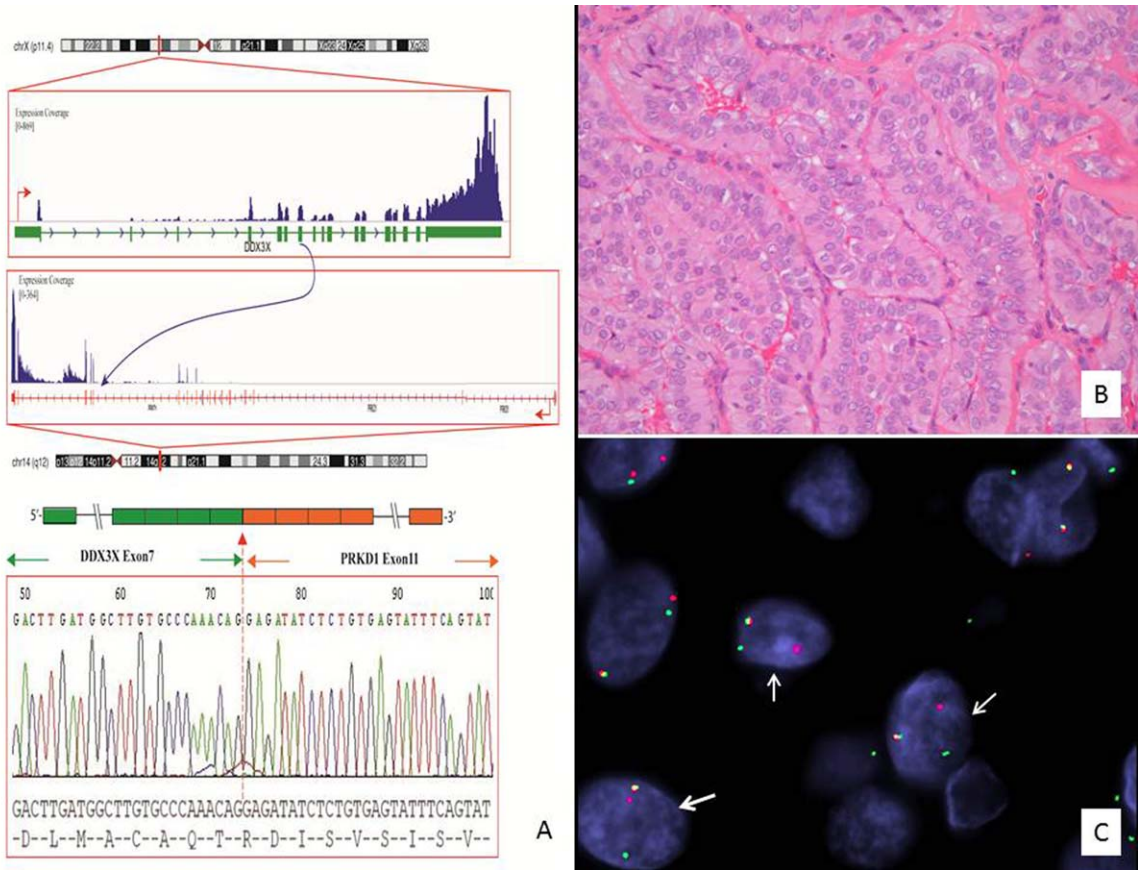

Figure 3. *DDX3X-PRKD1* gene fusion in a parotid cribriform adenocarcinoma of salivary gland (SA6). (A) Schematic representation of the *DDX3X-PRKD1* fusion indicating the loci that are joined together; *DDX3X* exon 7 being fused to *PRKD1* exon 11 (top image). Experimental validation of the fusion by RT-PCR shows the junction sequence between exon 7 of *DDX3X* and exon 11 of *PRKD1* (bottom image); (B) The index case SA6 showed some typical CAMSG morphology but also showed trabecular architecture with a columnar or "tall cell" appearance; (C) FISH for *DDX3X* shows break apart signals with one normal fused yellow signal and separate 5′ green and 3′ red signals indicating rearrangement of the gene (arrows). [Color figure can be viewed in the online issue, which is available at wileyonlinelibrary.com.]

distribution, including nasopharynx and parotid. Of the seven cases with known lymph node metastases, all were classified as CAMSG, six showed rearrangement of one of the *PRKD* genes and five were located in the base of tongue/pharynx. In fact all 10 cases occurring in pharynx (seven oropharynx and three nasopharynx) were positive for a *PRKD* rearrangement.

ARID1A-PRKD1 Induces Similar Transcriptional Abnormalities in a Normal Salivary Gland Cell Line (HPAM1) as Seen in fusion-positive CAMSG Tumors

Based on RNA sequencing data, we first selected 462 upregulated transcripts in the SA samples with the RPKM (Habegger et al., 2011) values above 100, compared to a wide range of other tumor types. We then applied information content for constructing sequence logos as an additional ranking parameter (Schneider and Stephens 1990), which identifies genes that have null expression in most samples except for the subset of interest (i.e., SA tumors). Log fold change between *PRKD1*-positive SA and all other tumors was the last ranking parameter. Based on these criteria, three top-ranked transcripts were identified: *CLDN10*, *CRISPLD1* and *MUC7* (Supporting Information Fig. 1). The mRNA expression of these genes was then investigated by real-time PCR in the normal salivary gland cells (HPAM1) as well as in the *ARID1A-PRKD1* transduced HPAM1. Two of the three genes analyzed, *CLDN10* and *MUC7*, showed increased expression exclusively in HPAM1 transduced with *ARID1A-PRKD1* (Supporting Information Fig. 1). Furthermore, real-time PCR performed on the HPAM1 expressing the *ARID1A-PRKD1* fusion transcript and corresponding controls showed significant upregulation of *PRKD1* mRNA (Supporting Information Fig. 2).

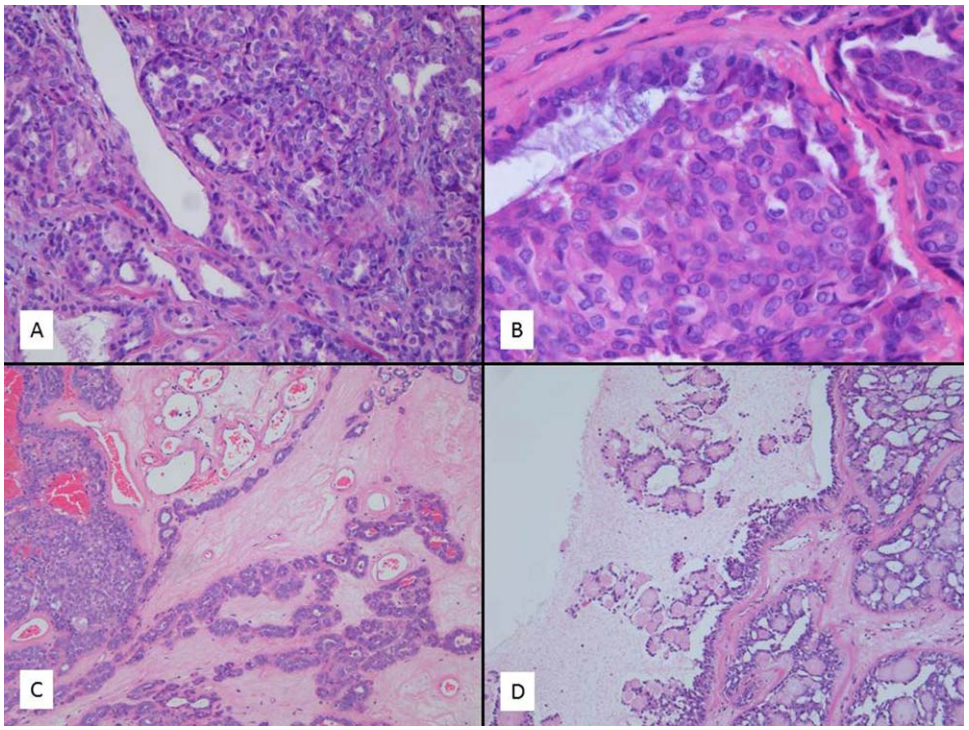

Figure 4. Variant morphologies in *PRKD1* rearranged tumors without *DDX3X* or *ARID1A*. (A, B) An indeterminate case showing tubular (A) and glomeruloid (B) features. One *PRKD1* rearranged tumor in the nasopharynx showed abundant canalicular like growth (C). Another tumor showed an unusual pattern of cribriform and papillary-cystic architecture (D). [Color figure can be viewed in the online issue, which is available at wileyonlinelibrary.com.]

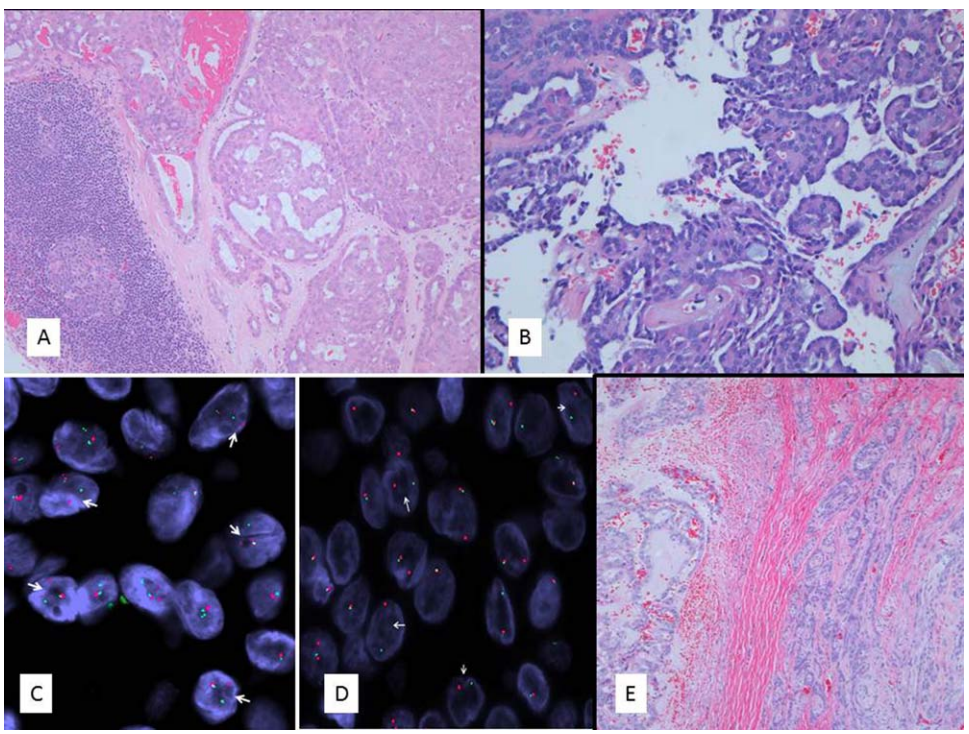

Figure 5. Most cases with *PRKD2* and *PRKD3* showed classic CAMSG morphology or indeterminate features (A, B). A lymph node metastasis of a *PRKD2* rearranged tumor is shown here with typical glomeruloid morphology (A). Another *PRKD3* rearranged CAMSG case with papillary features is shown here (B). *PRKD2* (C) and *PRKD3* (D) FISH for these cases showed classic break-apart signals. A single *PRKD2* rearranged case in the parotid (E) showed a classic PLGA targetoid/fascicular growth pattern (right) with foci of canalicular growth (left). [Color figure can be viewed in the online issue, which is available at wileyonlinelibrary.com.]

TABLE 1. Clinicopathologic Features of *PRKD1–3* Rearranged Tumors

Case#	Age/ sex	Location	Diagnosis	Morphologic patterns	*ARID1A* FISH	*DDX3X* FISH	*PRKD* FISH
1	38F	Buccal	CAMSG	Solid with slit-like spaces	Positive	ND	PRKD1
2[a]	49M	Base of tongue	CAMSG	Solid with slit-like spaces and glomeruloid	Positive	ND	PRKD1
3	65F	Base of tongue	CAMSG	Solid, glomeruloid, and papillary	Negative	Negative	PRKD3
4	75M	Palate	CAMSG	Solid, glomeruloid, and papillary	Negative	Negative	PRKD2
6[a]	46F	Parotid	CAMSG	Solid and papillary	Negative	Positive	PRKD1
7	52F	Floor of mouth	CAMSG	Solid, glomeruloid, and papillary	Positive	ND	Negative
8	76M	Base of tongue	CAMSG	Solid, cribriform, and glomeruloid	Negative	Negative	PRKD3
9	NA	Oropharynx	CAMSG	Glomeruloid and papillary	Fail	Negative	PRKD3
12	72F	Tongue	CAMSG	Solid with slit-like spaces and glomeruloid	Negative	Negative	PRKD1[b]
14	71M	Base of tongue	CAMSG	Solid with slit-like spaces and glomeruloid	Negative	Negative	PRKD3
15	26F	Base of tongue	CAMSG	Solid, glomeruloid, and papillary	Positive	ND	PRKD1
16	52F	Palate	CAMSG	Solid, glomeruloid, and papillary	ND	Negative	PRKD2
17	72M	Buccal	CAMSG	Solid with slit-like spaces and papillary	Negative	Negative	PRKD1[c]
18	64F	Palate	CAMSG	Solid and glomeruloid	Negative	Negative	PRKD1[d]
19	59F	Buccal	CAMSG	Solid and glomeruloid	Negative	Negative	PRKD1
21	29F	Nasopharynx	CAMSG	Solid and glomeruloid	ND	Negative	PRKD2
30	76F	Parotid	PLGA	Fascicular, targetoid, canalicular	Negative	Negative	PRKD2
40	84F	Tonsil	Indeterminate	Microcystic and cribriform	Negative	Negative	PRKD2
43	61M	Palate	Indeterminate	Fascicular, tubular, and focal glomeruloid	Negative	Negative	PRKD1[b]
44	72F	Palate	Indeterminate	Solid, tubular, and glomeruloid	Negative	Negative	PRKD3[c]
45	47F	Nasopharynx	Indeterminate	Solid, tubular, and glomeruloid	Negative	Negative	PRKD3
47	24M	Palate	Indeterminate	Tubular, cystic, cribriform, and papillary	Negative	Negative	PRKD1
48	62F	Palate	Indeterminate	Fascicular, tubular, and cribriform	Negative	Negative	PRKD1
54	75M	Lip	Indeterminate	Tubular and canalicular	Negative	Negative	PRKD2
55	61F	Nasopharynx	Indeterminate	Cribriform and canalicular	Negative	Negative	PRKD1
56	78F	Palate	Indeterminate	Tubular, cribriform, and glomeruloid	Negative	Negative	PRKD1

ND—not done; NA—not available.

[a]These cases represent the index tumors that were subjected to RNA sequencing. Case 2 showed an *ARID1A-PRKD1* fusion gene and case 6 showed a *DDX3X-PRKD1* fusion gene.

[b]These two cases showed a signal pattern consistent with an intrachromosomal rearrangement.

[c]These cases showed loss of the 5′ signal suggestive of an unbalanced translocation.

[d]This case showed a break in the 5′ telomeric signal outside the *PRKD1* gene.

Expression of Truncated PRKD1 Protein in ARID1A-PRKD1-Transduced Cells and a PRKD1-Rearranged CAMSG Tumor

Western blotting was performed on the *ARID1A-PRKD1* transduced NIH3-3T3 and corresponding controls, including NIH3-3T3 cells transduced with the empty vector, as well as the index case SA2, positive for the *ARID1A-PRKD1* fusion. The fusion-positive samples showed a 74 kDa size band, in keeping with truncated PRKD1 protein, in contrast to the 115 kDa wild type PRKD1 protein (Supporting Information Fig. 3). Additional samples, such as one angiosarcoma, one PEC-oma and three GISTs were included displaying only the 115 kDa wild type band (data not shown).

DISCUSSION

PLGA is a salivary gland cancer, which was first described by Evans and Batsakis (1984). PLGA is known for its heterogeneous architecture but uniform cytology (Evans and Batsakis, 1984). The tumors occur in women more often than men and most arise in the palate (Luna and Wenig, 2005). PLGAs are generally small and easily treated surgically and unlike the principal differential diagnosis, namely adenoid cystic carcinoma, they have an excellent prognosis with a small incidence of recurrence and cervical lymph node metastases overall (Castle et al., 1999; Seethala et al., 2010). Extrapalatal site has been linked to a more aggressive course (Seethala et al., 2010). Even when recurrent and metastatic, many PLGAs can still be cured and hematogenous spread and mortality are rare. Evans and Luna (2000) revisited the entity in a series of 40 cases with long term follow up in 2000 and found that papillary growth was one feature that could be associated with more cervical lymph node metastases, and although "low grade" there have been reports of adverse outcomes in PLGA (Perez-Ordonez et al., 1998; Castle et al., 1999) and occasional cases of "high grade transformation/dedifferentiation" (Simpson et al., 2002).

Despite its "polymorphous" pattern it was still considered one entity until recently. Michal et al. (1999) first described "cribriform adenocarcinoma of the tongue (CAT)". This tumor was felt to be unique in that it usually arose in the base of tongue, had cervical lymph node metastases at presentation, and had characteristically optically clear nuclei, reminiscent of papillary thyroid cancer. Despite this behavior, the prognosis was still excellent. However, the CAT entity was not universally accepted as its own entity and was considered a variant pattern of PLGA by the World Health Organization "blue book" classification of head and neck tumors (Luna and Wenig, 2005). A follow up paper from the same authors described a larger series of new cases in 2011, now under the appellation "cribriform adenocarcinoma of minor salivary gland origin (CAMSG)" (Skalova et al., 2011). This was considered its own entity, not just because of clinical presentation, but also based on the immunohistochemical and ultrastructural evidence of "myosecretory differentiation," which is absent in PLGA. Whether CAMSG will be accepted as unique in future classifications remains to be seen.

We have observed that many putative cases of CAMSG have papillary and glomeruloid structures, sometimes diffusely, which were seen only focally in the original descriptions of the entity (Michal et al., 1999; Skalova et al., 2011). We have hypothesized that these cases may in fact show the same papillary pattern that was first thought by Evans and Luna to represent a potential prognosticator for greater metastatic spread to lymph nodes in PLGA (Evans and Luna, 2000). To explore this controversial spectrum of tumors, further, we used next generation RNA sequencing on two candidate CAMSG cases and two classic PLGAs and analyzed the data using FusionSeq, which is a bioinformatics tool that has been proven to predict fusions using paired-end RNA sequencing data (Sboner et al., 2010; Antonescu et al., 2013; Mosquera et al., 2013). No candidate fusion was found in the two sequenced classic PLGAs. The index CAMSG case SA2 was predicted to have an *ARID1A-PRKD1* chimeric transcript and this was validated using RT-PCR and further confirmed by FISH. In addition, the index CAMSG case SA6 was found to have a *DDX3X-PRKD1* fusion, which was also confirmed by RT-PCR and FISH.

The FISH probes for *ARID1A* and *PRKD1* genes were then applied to a series of 60 cases that spanned the spectrum from typical CAMSG, classic PLGAs, and indeterminate/mixed cases. A total of 14 cases (24%) had rearrangement of *ARID1A* and/or *PRKD1*. Three cases showed both, suggesting an *ARID1A-PRKD1* fusion. These cases had identical morphology and were considered typical CAMSG cases. They occurred in base of tongue ($n = 2$) and buccal mucosa ($n = 1$). The CAMSG case with *DDX3X-PRKD1* occurred in the parotid and showed some unusual features, including areas of trabecular architecture with a "tall cell" appearance. An additional case of CAMSG showed only *ARID1A* rearrangement, while nine cases showed break-apart in *PRKD1*, without associated *ARID1A* or *DDX3X* rearrangements, four of which were typical CAMSG cases. In screening the remaining cases for *PRKD2* and *PRKD3* gene abnormalities by FISH, an additional six cases each showed *PRKD2* and *PRKD3* rearrangements. Of these, seven showed classic CAMSG morphology, four were indeterminate, and one was a possible PLGA.

A total of 16/20 (80%) typical CAMSG cases showed gene rearrangements in one of these genes, with 15/20 (75%) showing abnormalities in one of the *PRKD* genes. The indeterminate/mixed category showed 9/20 (45%) cases with rearrangements in one of these genes. On retrospective review of the fusion-positive cases, one new feature not seen in fusion-negative cases was canalicular architecture. This appearance has not been previously thought to be part of the CAMSG spectrum and requires further investigation. Otherwise no specific findings in the indeterminate group were predictive of fusion status. Remarkably, only one PLGA case had abnormalities in one of these genes, a parotid tumor with *PRKD2* rearrangement (1/18; 6%). Although the association of CAMSG histology with the presence of *PRKD* gene rearrangements is striking compared to classic PLGA, several limitations in our study preclude a definitive conclusion on CAMSG being a unique and distinctive entity.

The most apparent reason to use caution is due to the difficulty in the histologic classification encountered in up to one-third of cases. This diagnostic challenge was in keeping with the significant morphologic overlap shared by these two entities and the potential inclusion of these entities as part of a spectrum. In addition, a large percentage of the indeterminate category was positive for *PRKD* rearrangements and one potential parotid PLGA was positive for *PRKD2* as well. Although this latter case was an isolated example, it highlights the need for a larger number of cases

in all categories to explore the potential for these genes to be involved in classic PLGA as well.

ARID1A, *DDX3X*, and *PRKD* genes have not been implicated in a translocation/fusion previously and very little is known of the function of *PRKD* genes or their potential role in oncogenesis. *ARID1A* is a gene well known to be involved in chromatin remodeling and has been implicated in gynecological cancers previously (Wiegand et al., 2010). The loss of *ARID1A* function leads to aberrations in DNA repair. Interestingly, *DDX3X* is also a gene involved in DNA repair (Sun et al., 2013) and has been implicated in a number of cancers including medulloblastoma (Jones et al., 2012) and breast cancer (Botlagunta et al., 2008). This may provide an as yet unknown link between *DDX3X* and *ARID1A*, at least in terms of how promoter swapping may activate *PRKD1* in these tumors. The *PRKD1* gene encodes a kinase that has previously been implicated in colorectal, breast, esophageal, laryngeal, and other cancers, although deletion and/or gene silencing appear to be the mechanisms associated with colorectal and breast cancers (Borges et al., 2013; Brim et al., 2014), while activation is associated with esophageal and laryngeal cancers (Fountzilas et al., 2014; Xie et al., 2014). Along with the related *PRKD2* and *PRKD3* genes, it is associated with signal transduction in the diacylglycerol (DAG) and protein kinase C (PKC) pathway. When activated PRKD family of kinases have a role in signal transduction, trafficking, migration, differentiation and proliferation (Xie et al., 2014) and potentially may serve as targets for future drug therapies. Further studies are required to elucidate the mechanism of *PRKD* gene activation in these tumors and how this leads to tumor proliferation.

In summary, recurrent *PRKD1*, *PRKD2*, and *PRKD3* rearrangements, including *ARID1A-PRKD1* and *DDX3X-PRKD1* fusions, are associated with the "polymorphous low-grade adenocarcinoma (PLGA)/cribriform adenocarcinoma (CAMSG)" spectrum of salivary gland cancer. The fusion-positive group appears to cluster mainly in CAMSG and indeterminate cases rather than in "classic PLGA," however, a large percentage of cases in this spectrum remain uncharacterized genetically. The presence of *PRKD* gene abnormalities in indeterminate cases precludes using them as diagnostic markers or confirming the uniqueness of CAMSG at this time, although it appears to be the first evidence of a difference between CAMSG and "classic PLGA." Further sequencing studies of fusion-negative cases are required to identify additional genetic markers that may fill in this gap and larger annotated cohorts that include patient outcome are also required to address the potential role of *PRKD* with the alleged greater tendency for CAMSG to metastasize to cervical lymph nodes (Evans and Luna, 2000; Skalova et al., 2011).

REFERENCES

Antonescu CR, Zhang L, Chang NE, Pawel BR, Travis W, Katabi N, Edelman M, Rosenberg AE, Nielsen GP, Dal Cin P, Fletcher CD. 2010. EWSR1-POU5F1 fusion in soft tissue myoepithelial tumors. A molecular analysis of sixty-six cases, including soft tissue, bone, and visceral lesions, showing common involvement of the EWSR1 gene. Genes Chromosomes Cancer 49:1114–1124.

Antonescu CR, Katabi N, Zhang L, Sung YS, Seethala RR, Jordan RC, Perez-Ordoñez B, Have C, Asa SL, Leong IT, Bradley G, Klieb H, Weinreb I. 2011. EWSR1-ATF1 fusion is a novel and consistent finding in hyalinizing clear-cell carcinoma of salivary gland. Genes Chromosomes Cancer 50:559–570.

Antonescu CR, Le Loarer F, Mosquera JM, Sboner A, Zhang L, Chen CL, Chen HW, Pathan N, Krausz T, Dickson BC, Weinreb I, Rubin MA, Hameed M, Fletcher CD. 2013. Novel YAP1-TFE3 fusion defines a distinct subset of epithelioid hemangioendothelioma. Genes Chromosomes Cancer 52:775–784.

Borges S, Döppler H, Perez EA, Andorfer CA, Sun Z, Anastasiadis PZ, Thompson EA, Geiger XJ, Storz P. 2013. Pharmacologic reversion of epigenetic silencing of the PRKD1 promoter blocks breast tumor cell invasion and metastasis. Breast Cancer Res 23:R66.

Botlagunta M, Vesuna F, Mironchik Y, Raman A, Lisok A, Winnard P, Jr., Mukadam S, Van Diest P, Chen JH, Farabaugh P, Patel AH, Raman V. 2008. Oncogenic role of DDX3 in breast cancer biogenesis. Oncogene 27:3912–3922.

Brim H, Abu-Asab MS, Nouraie M, Salazar J, Deleo J, Razjouyan H, Mokarram P, Schaffer AA, Naghibhossaini F, Ashktorab H. 2014. An integrative CGH, MSI and candidate genes methylation analysis of colorectal tumors. PLoS One 27:e82185.

Castle JT, Thompson LD, Frommelt RA, Wenig BM, Kessler HP. 1999. Polymorphous low grade adenocarcinoma: A clinicopathologic study of 164 cases. Cancer 86:207–219.

Dobin A, Davis CA, Schlesinger F, Drenkow J, Zaleski C, Jha S, Batut P, Chaisson M, Gingeras TR. 2013. STAR: ultrafast universal RNA-seq aligner. Bioinformatics 29:15–21.

Evans HL, Batsakis JG. 1984. Polymorphous low-grade adenocarcinoma of minor salivary glands. A study of 14 cases of a distinctive neoplasm. Cancer 53:935–942.

Evans HL, Luna MA. 2000. Polymorphous low-grade adenocarcinoma: A study of 40 cases with long-term follow up and an evaluation of the importance of papillary areas. Am J Surg Pathol 24:1319–1328.

Fountzilas E, Kotoula V, Angouridakis N, Karasmanis I, Wirtz RM, Eleftheraki AG, Veltrup E, Markou K, Nikolaou A, Pectasides D, Fountzilas G. 2013. Identification and validation of a multigene predictor of recurrence in primary laryngeal cancer. PLoS One 8:e70429.

Habegger L, Sboner A, Gianoulis TA, Rozowsky J, Agarwal A, Snyder M, Gerstein M. 2011. RSEQtools: A modular framework to analyze RNA-Seq data using compact, anonymized data summaries. Bioinformatics 27:281–283.

Jones DT, Jäger N, Kool M, Zichner T, Hutter B, Sultan M, Cho YJ, Pugh TJ, Hovestadt V, Stütz AM, Rausch T, Warnatz HJ, Ryzhova M, Bender S, Sturm D, Pleier S, Cin H, Pfaff E, Sieber L, Wittmann A, Remke M, Witt H, Hutter S, Tzaridis T, Weischenfeldt J, Raeder B, Avci M, Amstislavskiy V, Zapatka M, Weber UD, Wang Q, Lasitschka B, Bartholomae CC, Schmidt M, von Kalle C, Ast V, Lawerenz C, Eils J, Kabbe R, Benes V, van Sluis P, Koster J, Volckmann R, Shih D, Betts MJ, Russell RB, Coco S, Tonini GP, Schüller U, Hans V, Graf N, Kim YJ, Monoranu C, Roggendorf W, Unterberg A, Herold-Mende C, Milde T, Kulozik AE, von Deimling A, Witt O, Maass E, Rössler J, Ebinger M, Schuhmann MU, Frühwald MC, Hasselblatt M, Jabado N, Rutkowski S, von Bueren AO, Williamson D, Clifford SC, McCabe MG, Collins VP, Wolf S, Wiemann S, Lehrach H, Brors B, Scheurlen W, Felsberg J, Reifenberger G, Northcott PA, Taylor MD, Meyerson M,

Pomeroy SL, Yaspo ML, Korbel JO, Korshunov A, Eils R, Pfister SM, Lichter P. 2012. Dissecting the genomic complexity underlying medulloblastoma. Nature 488:100–105.

Luna MA, Wenig BM. 2005. In: Barnes L, Eveson JW, Reichart P, Sidransky D, editors. WHO Classification of Tumours. Pathology and Genetics of Head and Neck Tumours. Lyon: IARC Press, pp 223–224.

Martins C, Fonseca I, Roque L, Ribeiro C, Soares J. 2001. Cytogenetic similarities between two types of salivary gland carcinomas: adenoid cystic carcinoma and polymorphous low-grade adenocarcinoma. Cancer Genet Cytogenet 15:130–136.

Michal M, Skálová A, Simpson RH, Raslan WF, Curík R, Leivo I, Mukensnábl P. 1999. Cribriform adenocarcinoma of the tongue: a hitherto unrecognized type of adenocarcinoma characteristically occurring in the tongue. Histopathology 35:495–501.

Mosquera JM, Sboner A, Zhang L, Chen CL, Sung YS, Chen HW, Agaram NP, Briskin D, Basha BM, Singer S, Rubin MA, Tuschl T, Antonescu CR. 2013. Novel MIR143-NOTCH fusions in benign and malignant glomus tumors. Genes Chromosomes Cancer 52:1075–1087.

Perez-Ordonez B, Linkov I, Huvos AG. 1998. Polymorphous low-grade adenocarcinoma of minor salivary glands: A study of 17 cases with emphasis on cell differentiation. Histopathology 32: 521–529.

Persson M, Andrén Y, Mark J, Horlings HM, Persson F, Stenman G. 2009. Recurrent fusion of MYB and NFIB transcription factor genes in carcinomas of the breast and head and neck. Proc Natl Acad Sci USA 106:18740–18744.

Quail MA, Kozarewa I, Smith F, Scally A, Stephens PJ, Durbin R, Swerdlow H, Turner DJ. 2008. A large genome center's improvements to the Illumina sequencing system. Nat Methods 5:1005–1010.

Sboner A, Habegger L, Pflueger D, Terry S, Chen DZ, Rozowsky JS, Tewari AK, Kitabayashi N, Moss BJ, Chee MS, Demichelis F, Rubin MA, Gerstein MB. 2010. FusionSeq: A modular framework for finding gene fusions by analyzing paired-end RNA-sequencing data. Genome Biol 11:R104.

Schneider TD, Stephens RM. 1990. Sequence logos: A new way to display consensus sequences. Nucleic Acids Res 18:6097–6100.

Seethala RR, Johnson JT, Barnes EL, Myers EN. 2010. Polymorphous low-grade adenocarcinoma: The University of Pittsburgh experience. Arch Otolaryngol Head Neck Surg 136:385–392.

Simpson RH, Pereira EM, Ribeiro AC, Abdulkadir A, Reis-Filho JS. 2002. Polymorphous low-grade adenocarcinoma of the salivary glands with transformation to high-grade carcinoma. Histopathology 41:250–259.

Skalova A, Vanecek T, Sima R, Laco J, Weinreb I, Perez-Ordonez B, Starek I, Geierova M, Simpson RH, Passador-Santos F, Ryska A, Leivo I, Kinkor Z, Michal M. 2010. Mammary analogue secretory carcinoma of salivary glands, containing the ETV6-NTRK3 fusion gene: A hitherto undescribed salivary gland tumor entity. Am J Surg Pathol 34:599–608.

Skalova A, Sima R, Kaspirkova-Nemcova J, Simpson RH, Elmberger G, Leivo I, Di Palma S, Jirasek T, Gnepp DR, Weinreb I, Perez-Ordoñez B, Mukensnabl P, Rychly B, Hrabal P, Michal M. 2011. Cribriform adenocarcinoma of minor salivary gland origin principally affecting the tongue: Characterization of new entity. Am J Surg Pathol 35:1168–1176.

Sun M, Zhou T, Jonasch E, Jope RS. 2013. DDX3 regulates DNA damage-induced apoptosis and p53 stabilization. Biochim Biophys Acta 1833:1489–1497.

Tonon G, Modi S, Wu L, Kubo A, Coxon AB, Komiya T, O'Neil K, Stover K, El-Naggar A, Griffin JD, Kirsch IR, Kaye FJ. 2003. t(11;19)(q21;p13) translocation in mucoepidermoid carcinoma creates a novel fusion product that disrupts a Notch signaling pathway. Nat Genet 33:208–213.

Wiegand KC, Shah SP, Al-Agha OM, Zhao Y, Tse K, Zeng T, Senz J, McConechy MK, Anglesio MS, Kalloger SE, Yang W, Heravi-Moussavi A, Giuliany R, Chow C, Fee J, Zayed A, Prentice L, Melnyk N, Turashvili G, Delaney AD, Madore J, Yip S, McPherson AW, Ha G, Bell L, Fereday S, Tam A, Galletta L, Tonin PN, Provencher D,Miller D, Jones SJ, Moore RA, Morin GB, Oloumi A, Boyd N, Aparicio SA, Shih IeM, Mes-Masson AM, Bowtell DD, Hirst M, Gilks B, Marra MA, Huntsman DG. 2010. ARID1A mutations in endometriosis-associated ovarian carcinomas. N Engl J Med 363:1532–1543.

Xie X, Zhang SS, Wen J, Yang H, Luo KJ, Yang F, Hu Y, Fu JH. 2014. Protein kinase D1 mRNA level may predict cancer-specific survival in heavy smokers with esophageal squamous cell cancers. Dis Esophagus 27:188–195.